

Optical Engineering

OpticalEngineering.SPIEDigitalLibrary.org

Accuracy analysis of indoor visible light communication localization system based on received signal strength in non-line-of-sight environments by using least squares method

Ge Shi
Yong Li
Wei Cheng
Limeng Dong
Junhua Yang
Wenjie Zhang

SPIE.

Ge Shi, Yong Li, Wei Cheng, Limeng Dong, Junhua Yang, Wenjie Zhang, "Accuracy analysis of indoor visible light communication localization system based on received signal strength in non-line-of-sight environments by using least squares method," *Opt. Eng.* **58**(5), 056102 (2019), doi: 10.1117/1.OE.58.5.056102.

Accuracy analysis of indoor visible light communication localization system based on received signal strength in non-line-of-sight environments by using least squares method

Ge Shi, Yong Li,* Wei Cheng, Limeng Dong, Junhua Yang, and Wenjie Zhang

Northwestern Polytechnical University, School of Electronics and Information, Xi'an, China

Abstract. For an indoor localization system based on visible light communication (VLC) by using received signal strength technique, visible light signals used for estimating the distances between each localization target and reference nodes suffer from non-line-of-sight (NLoS) signal propagation, which could introduce large errors in estimating their locations. Both line-of-sight (LoS) link and NLoS link are taken into account in a noisy VLC channel, and thus the NLoS signal and ambient noise are the sources of localization error. Ricean K factor is introduced to evaluate the relation between the value of NLoS signal and the quality of localization in the proposed system. Analytical expressions for the distance measurement error and the upper bound of localization error are derived by using the least squares method. The simulation results show that the estimation of localization error matches the distribution of Ricean K factor in the noisy overall link. The environmental parameters that can be used to decrease the value of Ricean K factor are also discussed in the simulations, which provide the reference of parameters for building an experimental demonstration of a VLC indoor localization system. A comparison is conducted with the previous works to demonstrate the good performance of our scheme.

© The Authors. Published by SPIE under a Creative Commons Attribution 4.0 Unported License. Distribution or reproduction of this work in whole or in part requires full attribution of the original publication, including its DOI. [DOI: [10.1117/1.OE.58.5.056102](https://doi.org/10.1117/1.OE.58.5.056102)]

Keywords: visible light communication; receiver signal strength; least squares method; non-line-of-sight link.

Paper 181849 received Jan. 5, 2019; accepted for publication Apr. 10, 2019; published online May 8, 2019.

1 Introduction

With the continuous increase of location-aware wireless applications, various indoor localization techniques based on radio frequency (RF) electromagnetic waves,^{1,2} ultrasound,³ and infrared⁴ (IR) have been proposed. For low-frequency RF-based approaches, such as wireless local networks^{4,5} (WLAN) and ultra-wideband,⁶ the localization accuracy is highly related to the density and distribution of the routers, and the wireless RF signals are liable to suffer from RF interference.⁷ The average localization error for RF localization is several meters, and this accuracy level cannot be applied to the traditional tri-angulation process to localize user devices correctly due to multipath propagation.⁸ Ultrasound-based approaches can provide a high localization accuracy of 10 cm but require expensive and specialized infrastructures.⁹ IR-based indoor localization can achieve relatively high localization accuracy of centimeter-level, but its transmission distance (1 m) is shorter than that of VLC (10 m).¹⁰ It also leads to a higher cost since it is necessary to install large numbers of IR nodes in the room. Recently, visible light communication (VLC) localization methods have drawn much attention of researchers and industries. Unlike conventional techniques, VLC-based localization is immune to electromagnetic interference and can be used in RF-restricted zones¹¹ (e.g., airport and hospital). It can achieve centimeter-level accuracy¹²⁻²² with lower cost infrastructures by remodifying the existing illumination system to VLC transmitters. Moreover, it offers a higher security for users

since visible light signals cannot transmit across the walls and may not be accessed by eavesdroppers from other rooms.¹²

Owing to these advantages, several schemes have been proposed by researchers to realize visible light localization based on the techniques of time of arrival (TOA),¹³ angle of arrival,¹⁴ and received signal strength (RSS) indicator. VLC localization based on TOA and time difference of arrival¹⁵ required strict synchronization between transmitters, as the distances between the receivers and the transmitters in indoor applications are generally short. In Ref. 16, a receiver, which was installed on a rotatable and retractable platform, was proposed in a three-dimensional (3-D) indoor VLC localization system. According to the difference of angle gains measured by rotating the receiver platform, a 3-D localization algorithm was proposed, and the experiments showed that the average localization error was <35 mm in the indoor environment. Zhu et al.¹⁷ proposed a 3-D localization framework based on the angle differences of arrival (ADOAs), and an arbitrary tilting angle of receiver was used to extract the information of ADOA. Both analytical results and experimental results show that an average error of 3.2 cm can be achieved by the least squares method in this framework. The VLC localization methods based on ADOA can achieve millimeter-level accuracy. However, compared to the approaches based on RSS technique, it acquired a platform to tilt and rotate the receiver to different azimuth angles, which may increase the cost of production and time of measurements.

In this study, we have focused on the VLC localization system based on the RSS technique because this scheme

*Address all correspondence to Yong Li, E-mail: ruikeli@nwpu.edu.cn

is simple to realize and does not need synchronization between the transmitter and the receiver, or a specialized platform to rotate the receivers. In Ref. 18, a RSS-based VLC localization system combined with RF carrier allocation technique was proposed, and an average localization error of 2.4 cm was achieved. Reference 19 reported an RSS-based localization approach based on the bounding-box algorithm to enhance the accuracy of the VLC localization system in a noisy line-of-sight (LoS) environment. These works only considered the LoS channels and neglected the effect of diffuse reflection on the performance of the VLC localization system. However, non-line-of-sight (NLoS) components should be considered in the analysis of accuracy since large positive errors were introduced in the localization systems when employing the VLC propagation models. In Ref. 20, an iterative localization algorithm based on bilinear interpolation was proposed to subtract the diffuse reflection from the received signals, and the average error could be reduced by 12 times with only two iterations. Two lighting systems were investigated in Ref. 21, and the results showed that uniform lighting systems achieve a better localization performance than the discrete ones in a scenario including NLoS signals. These two works analyzed the effects of NLoS component on the accuracy of VLC indoor localization only through simulations. However, theoretical accuracy analysis of the indoor VLC localization system based on RSS has been seldom conducted. In Ref. 22, a mathematical relation between the measured distance error and the signal-to-noise ratio (SNR) was obtained. However, a mathematical expression which revealed the relation between the localization error and the value of NLoS components in this scenario has not been obtained yet. We aimed to reveal the relation between the localization error and the value of NLoS components by introducing K factor through both analysis and simulations in a typical $5 \times 5 \times 3$ room installed with VLC equipment based on RSS and to increase the accuracy of the localization system by increasing the Ricean K factor in the simulations. More precisely, the following have been performed:

- We introduced Ricean K factor to express the relative power of LoS and NLoS signals in the total received power, which revealed the communication quality in the noisy overall link. Based on the propagation models, the mathematical relationship between the K factor and measured distance error was explored.
- By solving a group of equations using the linear least squares method, we obtained an upper bound of the localization error which was inversely proportional to the values of K factor and SNR at an arbitrary receiver position and positively proportional to the propagation distance.
- To reduce the localization error, we took several measurements to enhance the SNR and Ricean K factor of the VLC link. The simulation showed that these methods can improve the localization accuracy to a millimeter-level.

The rest of this paper is organized as follows: Sec. 2 represents VLC channel modeling for both LoS and NLoS scenarios. Section 3 outlines the localization problem in this work. In Sec. 4, simulations for the distribution of signal

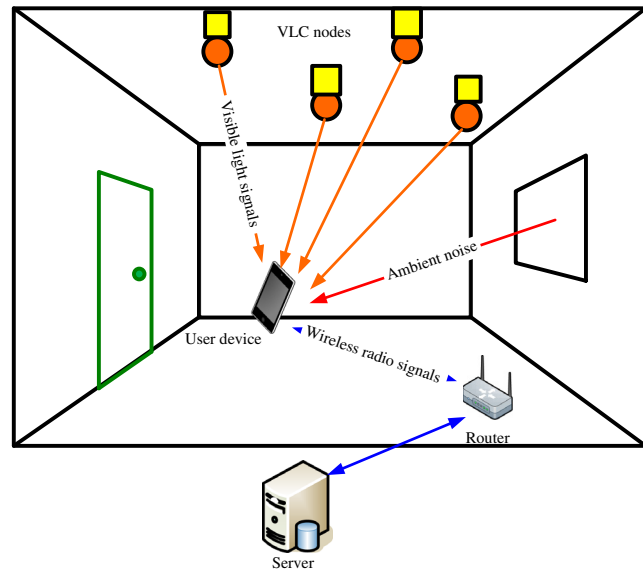


Fig. 1 VLC indoor localization system.

strength, K factor, and localization error are conducted all over the room, and the results corresponding to different parameters in the system are demonstrated. Finally, the conclusions are drawn in Sec. 5.

2 Visible Light Communication System Modeling

As shown in Fig. 1, a VLC localization system is composed of four parts, including VLC nodes, a user device, a router, and a server. The VLC nodes, which are fixed on the ceiling of the office, are used to broadcast visible light signals with location information to the room. A user device receives visible light signals from nodes by using a photodiode (PD) and extracts the information (ID number of nodes, RSS) from the signals. Next, the user further communicates with a router in the room and uploads the information of all received VLC signals to a server. The server stores a list that indicates the one-to-one relationship between the ID numbers and the coordinates for every node. By modeling the characteristics of the VLC channel, the distances between the user device and the VLC nodes can be measured by the RSS technique, and the user position can be estimated by the least squares method. The distance measurement and localization estimation are conducted in the server and the result will be sent to the user device and shown to the user by an application. In this scenario, both the LoS and the NLoS links should be taken into account in distance measurement because the localization system based on RSS is sensitive to NLoS signals. Furthermore, the characteristics of the VLC channel are affected considerably by both the system hardware and the application environment, and thus impact the quality of localization.

2.1 Line-of-Sight Channel Modeling

The PD receives the optical signal from the direct channel of the VLC system and converts it to electrical signal. The output electrical power P_e can be expressed as²¹

$$P_e = \begin{cases} \left[P_t \frac{\gamma A_r}{d^2} R(\phi) T(\varphi) g(\varphi) \cos(\varphi) \right]^2, & 0 \leq \varphi \leq \text{FOV} \\ 0 & \varphi \geq \text{FOV} \end{cases}, \quad (1)$$

where P_t is the average transmitted power, A_r is the physical area of detector, d is the distance between the transmitter and the receiver, $T(\varphi)$ is the optical filter gain, $g(\varphi)$ is the concentrator gain, FOV is the receiver's field of view, γ is the response rate of the PD, and $R(\phi)$ is the radiant angle intensity at radiation angle ϕ with respect to the receiver. In this system, light-emitting diode (LED) light source acts as an optical transmitter and its radiation pattern approximates to the Lambertian model; so, $R(\phi)$ can be modeled as $R(\phi) = [(m+1)/2\pi] \cos^m(\phi)$, where m is the mode number and is related to the transmitter's semiangle at half-power $\phi_{1/2}$. Thus, the distance between the transmitter and the receiver can be expressed as¹²

$$d = \left\{ \frac{[\gamma P_t (m+1) A_r h^{m+1} T_f(\varphi) g(\varphi)]^2}{4\pi^2 P_e} \right\}^{\frac{1}{6+2m}}, \quad (2)$$

where h is the vertical distance from the ceiling to the receiver.

2.2 Non-Line-of-Sight Optical Channel Modeling

Considering the scenario in Fig. 2 where light is reflected on the wall and reaches the receiver via a different path, the

$$\delta_1^2 = \begin{cases} \int_S \frac{\rho P_t A_r}{D_1^2 D_2^2} T(\varphi) g(\varphi) \cos^m(\phi) \cos(\alpha) \cos(\beta) \cos(\varphi) ds, & 0 \leq \varphi \leq \text{FOV} \\ 0 & \varphi \geq \text{FOV} \end{cases}, \quad (3)$$

where D_1 is the distance between the LED and the reflective area, D_2 is the distance between the reflective area and the receiver, and ρ is the reflectance factor depending on the material of reflective surface. When calculating the diffuse power reflected all around the walls, it is necessary to integrate through the whole reflective surface. Irrespective of how many times the light is reflected, the incident angle must be less than the FOV; otherwise the user device cannot receive the reflected signal. As the number of reflections increase, the length of the transmission path increases and the signal power decays gradually. In this paper, we only consider the first reflection signal as the NLoS component is degraded severely at the second reflection and can be neglected.²² Since the multipath reflected signal is still received by the device, it is very likely that the measured distance calculated by the RSS technique is greater than the actual value.

3 Mathematical Analysis of Localization Errors

In this section, we consider a typical VLC room where there are multiple LED nodes on the ceiling that transmit location data and one detector such as a mobile phone, pad, or PC to capture the signals. The coordinates of the transmitter are extracted from the received signals by the detector, and the distance between the transmitters and the detector is estimated by measuring the RSS of received signals. By using the least squares method, the user's location is obtained from

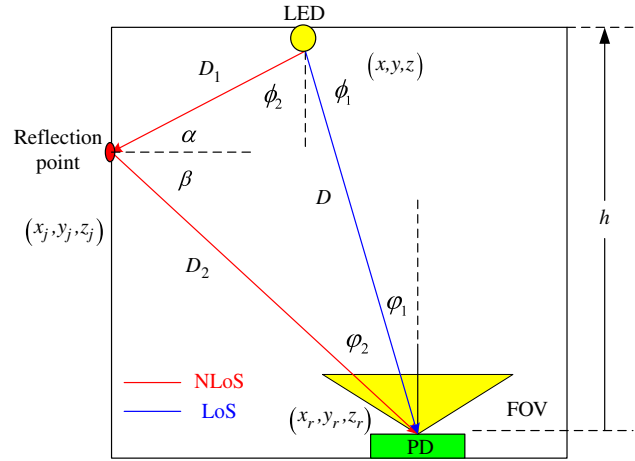


Fig. 2 Geometry of LoS and NLoS channels.

NLoS component should be taken into account in determining the total received power of a user device.

In this work, we first consider the diffuse component given by the sum of large numbers of multipath components, constituting a Gaussian process. Without loss of generality, we assume that the power of the diffuse component is δ^2 , and the reflective surface of the objects is divided into several small blocks, each of which satisfies the Lambertian luminance model. The received optical power δ_1^2 , which is reflected on the first reflection channel by a small reflective area dA , can be expressed as²¹

a set of equations which includes the required coordinates and estimated distances.

3.1 Analysis of Measured Distance Error

In practical scenarios, RSS-based localization systems are susceptible to noise and multipath propagation, and thus the total optical power received consist of three components: LoS signals, NLoS signals, and ambient noise. The total optical received power can be denoted as

$$P_r = P_d + P_f + P_n, \quad (4)$$

where P_n is the power of Gaussian additive noise $n \sim CN(0, P_n)$, which arise from thermal noise, dark current, and background radiation.²² According to Eq. (4), the measured distance d' can be rewritten as a sum of an error distance and actual distance

$$d' = d + \Delta d = \sqrt{\frac{m+3}{P_r} G(\varphi)}, \quad (5)$$

where $G(\varphi) = \frac{\gamma P_t (m+1) A_r h^{m+1} T_f(\varphi) g(\varphi)}{2\pi}$ is a variable that only corresponds to the position of the receiver. By substituting Eq. (4) into Eq. (5), the measured distance error Δd can be expressed as

$$\begin{aligned}\Delta d &= \sqrt[m+3]{\frac{G(\varphi)}{P_d}} - \sqrt[m+3]{\frac{G(\varphi)}{P_d \left(1 + \frac{P_f}{P_d} + \frac{P_m}{P_d}\right)}} \\ &= \sqrt[m+3]{d} \left(1 - \sqrt[m+3]{\frac{1}{1 + K^{-1} + \text{SNR}^{-1}}}\right).\end{aligned}\quad (6)$$

Evidently, the measured distance error is directly proportional to the actual distance between the receiver and the transmitter, whereas it is inversely proportional to the value of the K factor and SNR.

$$\begin{aligned}K = P_d/P_f &= \frac{P_t \frac{A_r}{D^2} R(\phi_1) T(\varphi_1) g(\varphi_1) \cos(\varphi_1)}{\int_S \frac{\rho P_t A_r}{D_1^2 D_2^2} T(\varphi_2) g(\varphi_2) \cos^m(\phi_2) \cos(\alpha) \cos(\beta) \cos(\varphi_2) ds} \\ &= \frac{h^2}{\rho D^4} \left[\int_S \frac{(h - z_s)(z_s - h + 5) \sqrt{(x - x_s)^2 + (y - y_s)^2} \sqrt{(x_r - x_s)^2 + (y_r - y_s)^2}}{D_1^4 D_2^4} ds \right]^{-1} \\ &= \frac{h^2}{\rho D^4} \left[\int_S \frac{(h - z_s)(z_s - h + 5) \sqrt{(x - x_s)^2 + (y - y_s)^2} \sqrt{(x_r - x_s)^2 + (y_r - y_s)^2}}{D_1^4 D_2^4} ds \right]^{-1} \\ &= \frac{h^2 \Delta S}{\rho D^4} \left[\sum_j \frac{(h - z_j)(z_j - h + 5) \sqrt{D_1^2 - (z - z_j)^2} \sqrt{D_2^2 - (z_r - z_j)^2}}{D_1^4 D_2^4} \right]^{-1},\end{aligned}\quad (7)$$

where S represents the total surface area of the reflectors in the room, and ds denotes a small reflection segment on the reflector surface located at (x_j, y_j, z_j) in the room. The VLC signal is reflected by this small area and then received by a user device placed at (x_r, y_r, z_r) . In Eq. (7), the receiver height h and reflectivity ρ are the two environmental parameters that can be assumed constant. Except for these parameters, the value of Ricean K factor is related to the relative positions of receiver, transmitters, and reflection objects. If the transmitters and reflection objects are arranged at fixed locations, the Ricean K factor only varies with the position of the receiver. Ricean K factor is inversely proportional to the LoS link length and positively proportional to the NLoS link length, but it is difficult to obtain a closed form expression of Ricean K factor in this configuration, since it is derived from the sum of all reflection components from four walls.

3.3 Upper Bound for Localization Error

In this section, we outline the traditional least squares-based method for localization and analyze its performance in the presence of overestimated distances due to the NLoS signal propagation. According to the geometric properties, at least three of the light sources are considered to be located at the center of a circle, and the measured distances are the radius of the circle. These three circles intersect at one point which is the measured position of the user device. The i 'th light source is installed at (x_i, y_i, z_i) , and the unlocalized user device is placed at (x, y, z) . All the transmitters are installed on the ceiling at the same height, and the user device is placed on the receiver plane h ; hence, the equation can be simplified to two dimensions as

3.2 Ricean K Factor

In the VLC system, the received signal can be expressed as the sum of a complex exponential and a narrowband Gaussian signal, which are known as the LoS component and diffuse component, respectively. The power ratio of the LoS component to the diffuse component is defined as the Ricean K factor which indicates the relative strength of the LoS²³ component. It is used to evaluate the accuracy of the measured distance in this configuration. As shown in Eq. (7), the Ricean K factor can be expressed as

$$\begin{aligned}(x_r - x_1)^2 + (y_r - y_1)^2 + h^2 &= d_1^2 \\ (x_r - x_2)^2 + (y_r - y_2)^2 + h^2 &= d_2^2 \\ &\vdots \\ (x_r - x_n)^2 + (y_r - y_n)^2 + h^2 &= d_n^2.\end{aligned}\quad (8)$$

This nonlinear equation group can be linearized by subtracting one of the equations from remaining $n - 1$ equations and the only unknown variables x and y in the above group of equations are the coordinates of the unlocalized device. These can be solved as a well-known problem using the linear least squares method, and thus $\mathbf{x} = (x_r, y_r)^T$ has a closed form solution given as

$$\mathbf{x} = (\mathbf{A}^T \mathbf{A})^{-1} \mathbf{A}^T \mathbf{b}.\quad (9)$$

If $\hat{\mathbf{b}}$ is a vector created by using the measured distances in Eq. (8), $\hat{\mathbf{x}}$ is obtained as an estimated solution, and the localization error can be given as a Euclid norm of the difference between $\hat{\mathbf{x}}$ and \mathbf{x}

$$\|\hat{\mathbf{x}} - \mathbf{x}\|_2 = \|(\mathbf{A}^T \mathbf{A})^{-1} \mathbf{A}^T \hat{\mathbf{b}} - (\mathbf{A}^T \mathbf{A})^{-1} \mathbf{A}^T \mathbf{b}\| \leq \|\mathbf{A}^\dagger\| \|\hat{\mathbf{b}} - \mathbf{b}\|,\quad (10)$$

where

$$\mathbf{A} = 2 \begin{bmatrix} (x_1 - x_n) & (y_1 - y_n) \\ (x_2 - x_n) & (y_2 - y_n) \\ \vdots & \vdots \\ (x_{n-1} - x_n) & (y_{n-1} - y_n) \end{bmatrix},\quad (11)$$

where \mathbf{A}^\dagger is the pseudoinverse of \mathbf{A} , and it is a constant if the placement of LED lamps are fixed in the room, because \mathbf{A} is only required by the distribution of transmitters. Based on the matrix theory, if \mathbf{A} is an ill-conditioned matrix, which has a higher conditional number, the whole localization system become more unstable. A small error in the measurement leads to a large derivation for the estimation of the receiver position $\hat{\mathbf{x}}$. Thus, the designer should pay attention to the distribution of VLC nodes. The difference between the actual distance and the measured ones which is the quality of localization is expressed as

$$\begin{aligned} \|\mathbf{b} - \hat{\mathbf{b}}\| &= \left[\sum_{i=1}^{n-1} (\Delta d_i^2 + 2d_i \Delta d_i - \Delta d_n^2 + 2d_n \Delta d_n)^2 \right]^{1/2} \\ &= \left\{ \sum_{i=1}^{n-1} \left[d_i^2 \left(1 - \sqrt{\frac{1}{1 + K_i^{-1} + \text{SNR}_i^{-1}}} \right)^2 \right. \right. \\ &\quad + 2d_i^{\frac{5}{2}} \left(1 - \sqrt{\frac{1}{1 + K_i^{-1} + \text{SNR}_i^{-1}}} \right) \\ &\quad - d_n^{\frac{1}{2}} \left(1 - \sqrt{\frac{1}{1 + K_n^{-1} + \text{SNR}_n^{-1}}} \right)^2 \\ &\quad \left. \left. - 2d_n^{\frac{5}{2}} \left(1 - \sqrt{\frac{1}{1 + K_n^{-1} + \text{SNR}_n^{-1}}} \right) \right]^2 \right\}^{1/2}, \quad (12) \end{aligned}$$

where Δd_i is the measured distance error between the user device and the i 'th light source. Equation (12) suggests that lower values of K factor and SNR significantly increase the vector norm $\|\mathbf{b} - \hat{\mathbf{b}}\|$ and thus raise the upper bound of localization error. The simulations conducted in Sec. 4 will further indicate the effect of these two factors on the localization system.

4 Stimulation Results and Discussion

This section describes the system characteristics and the simulation results obtained in the proposed work, starting with the received signal power distribution for the LoS link, NLoS link, and overall link, and followed by the distributions for SNR and K factor. Then, the distributions for localization error around the room are presented, and the effects of NLoS components and ambient noise are also discussed. Furthermore, the localization error under the different values of transmitter power, FOV of receiver, and wall reflectivity factors are presented. Finally, a comparison is made with the previous works, and the good performance of the proposed localization scheme is demonstrated.

4.1 System Characteristics

The size of the VLC room is $5 \times 5 \text{ m}^2$ with height of 3 m, and it is assumed to be empty except for a lighting system and a detector in it. The detector is placed at the plane of 0.85 m above the floor. The lighting system consists of four VLC nodes, each containing 60×60 LED chips which are arranged at the ceiling. A PD is contained in the detector, and it could receive the location code if optical light is incident within its FOV. Intensity modulation and direct detection is utilized in this VLC system due to its simple Implementation. Table 1 presents the simulation parameters considered for this work.

Table 1 Simulation parameters for the VLC system.

Parameters	Value
Room size	$5 \times 5 \times 3 \text{ m}^3$
Noise power P_n	0.01 m W
Wall reflectivity ρ	0.01
FOV	65 deg
Reflecting element area ds	1 cm^2
Surface area of the PD A_r	1 cm^2
Receiver plane h	0.85 m
Number of lights	4
Number of LEDs	60×60
Lambertian mode m	1
LED transmitter power P_t	50 m W/1 W
Response rate of PDs r	0.4 W/cm^2
Optical filter gain T	1
Concentrator gain g	1
Transmitter positions (x_i, y_i, z_i)	(1.25, 1.25, 3), (3.75, 3.75, 3), (3.75, 1.25, 3), (1.25, 3.75, 3)

4.2 Signal Power Distribution

The distributions of the received power at the detector level in the LoS and NLoS links are shown in Fig. 3. The simulation steps of LoS signal power distribution are as follows: (1) divide the surface of detector plane into small segments, and place a receiver at the center of every segment; (2) calculate Euclidean distances D between the receiver and the four transmitters; (3) apply distances and parameters in Table 1 to the mathematical model shown in Eq. (1) in order to get optical signal powers from the four transmitters; (4) the total LoS signal power at the receiver is required by adding all the optical signal powers together; (5) repeat steps from (1) to (4) and calculate the values of the LoS signal power from all the segments.

The simulation steps of the NLoS signal power distribution is similar to that of the LoS signal power but still have some following differences: (1) divide the surface of the detector plane into small segments and place a receiver at the center of every segment; (2) divide the four walls into small segments and place a reflective point at each wall segment; (3) calculate Euclidean distance between the receiver and the reflective point and distances between the reflective point and the four transmitters; (4) apply calculated distances and parameters in Table 1 to the mathematical model shown in Eq. (2) in order to get the NLoS signal power; (5) repeat steps from (3) to (4) to obtain the sum of the diffuse signal powers generated from four transmitter at the reflective point; (6) repeat steps from (2) to (5), and obtain the sum of NLoS signal powers from the four walls; (7) repeat steps from (1) to (5) and calculate the values of LoS signal power from all the segments.

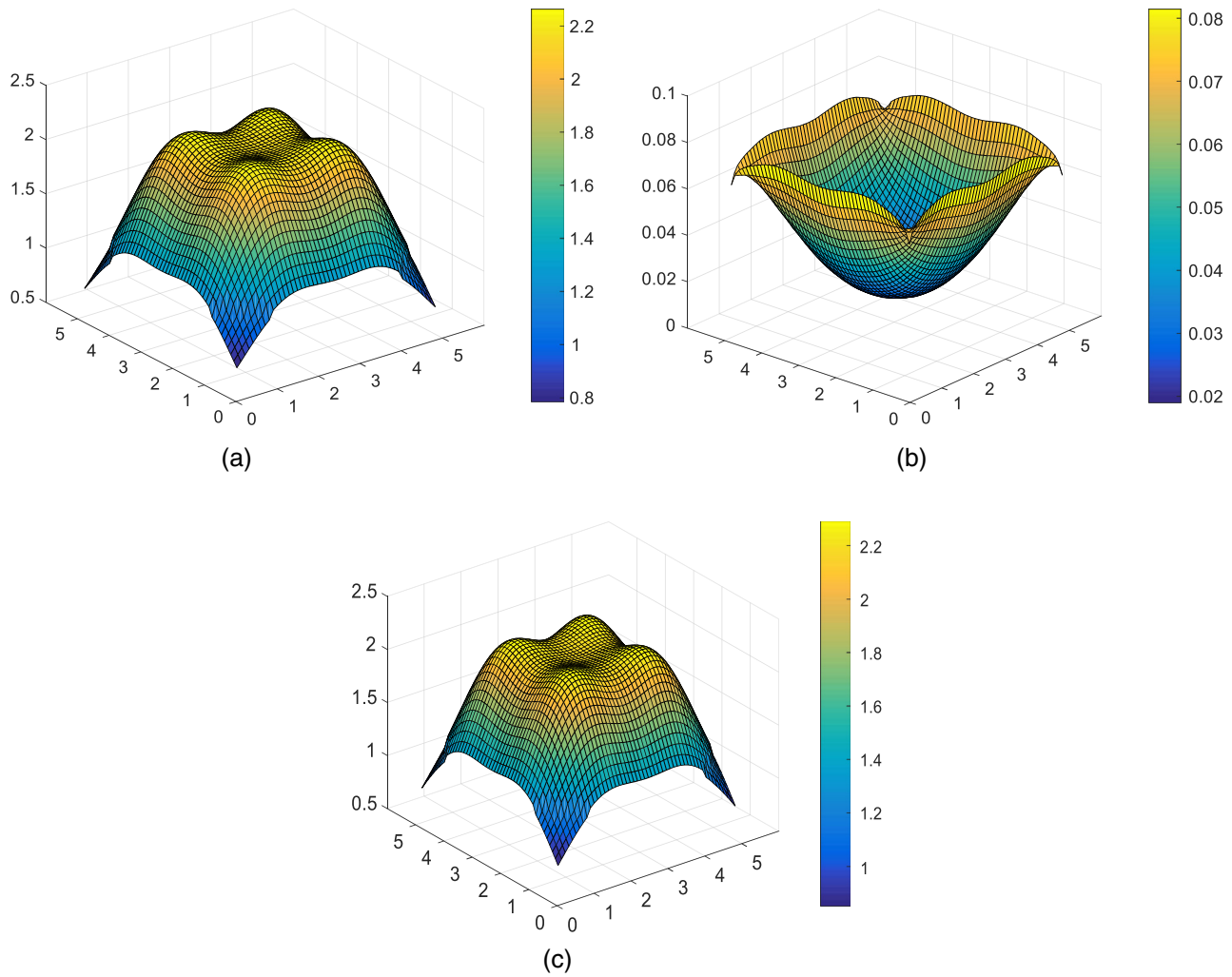


Fig. 3 RSS (mW) from (a) LoS link, (b) NLoS link, and (c) overall link.

As shown in Fig. 3(a), the value of LoS signal power is strongest under the positions of VLC transmitters. It gradually decreases from 2.26 to 0.78 mW when user moves from the positions of VLC transmitters to the four corners of the room. Figure 3(b) indicates that most of the NLoS components are concentrated near the walls, which makes the total power received by the detector on the walls to increase slightly by 0.08 mW. The minimum value of diffuse signal power is at the center of the room. Since the detector also absorbs NLoS signal power, it makes the total power received by detectors in the room to increase by 0.05 mW on the average. The received power of NLoS leads to an overestimation of distances and further damages the

accuracy in the localization process. Table 2 presents some details of Fig. 3 about the signal power received in the LoS, NLoS, and overall links, including the values of maximum, minimum, and average signal power and the corresponding coordinates. Only parts of the coordinates are shown in the table, since the result of simulation is central symmetry, e.g., the maximum values of the diffuse signal strength are also at (3.7, 0.1, 0.85), (1.3, 0.1, 0.85), and (0.1, 3.7, 0.85).

4.3 Distribution of K Factor

In the overall noisy link, the noise power acts as an extra part of the received power. As an index to show the quality

Table 2 Details of RSS from three different links.

Parameters	LoS power		Diffuse power		Total power	
	RSS/mw	Coordinate/m	RSS/mw	Coordinate/m	RSS/mw	Coordinate/m
Maximum	2.26	(1.6, 1.6, 0.85)	0.08	(0.1, 1.3, 0.85)	2.29	(1.5, 1.5, 0.85)
Minimum	0.78	(0.1, 0.1, 0.85)	0.02	(2.5, 2.5, 0.85)	0.85	(0.1, 0.1, 0.85)
Average	1.80		0.05		1.85	

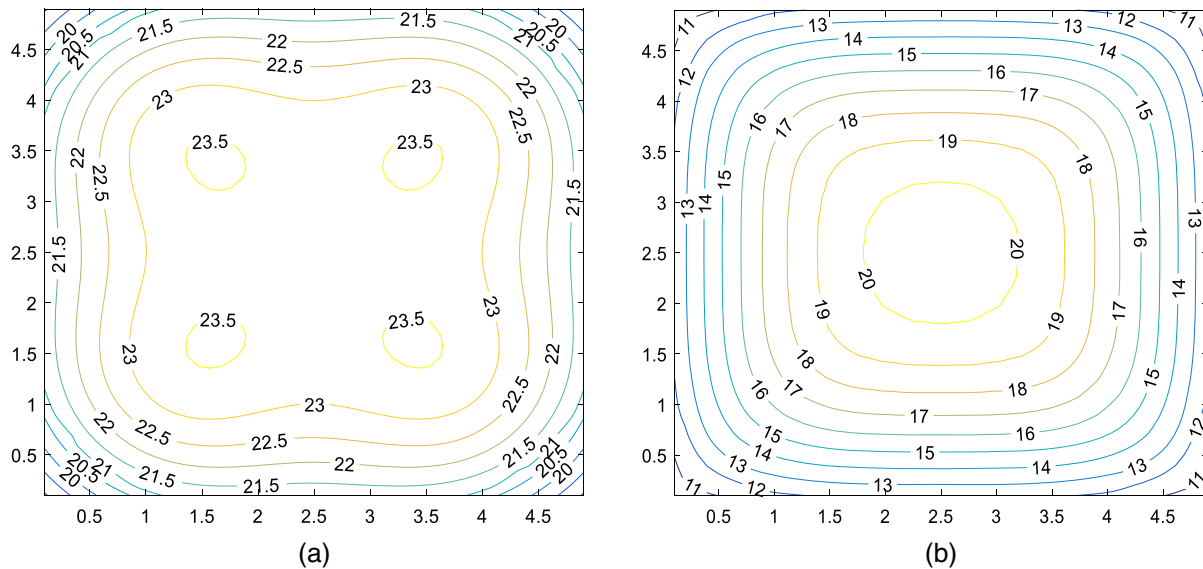


Fig. 4 Distribution of (a) SNR (dB) and (b) K factor (dB).

of communication in the noisy LoS link, SNR is defined as the ratio of LoS signal strength and Gaussian noise strength. Figure 4(a) indicates that the distribution of SNR is similar to that of the total received power in the overall link. The SNR of the VLC system starts to deteriorate as the user moves from the transmitter positions (SNR = 19.96 dB) to the four corners which is the worst scenario (SNR = 23 dB).

In the noisy overall link, the diffuse signal is another part of the received power. Not only Ricean K factor is a parameter to show the relative NLoS signal strength, but it is also a key parameter to indicate the accuracy of the VLC localization system in the NLoS environment. As shown in Fig. 4(b), the maximum value of the Ricean K factor is at the center of the room ($K = 20.54$ dB), and the worst scenarios occur at the corners ($K = 10.64$ dB). The distribution of Ricean factor is different from that of the signal received in the overall link because less diffuse signal lies at the center of the room, while most of the diffuse signal concentrates on the walls. Table 3 presents some details from Fig. 4, including the maximum, minimum, and average values and the corresponding coordinates.

4.4 Localization Error Distribution

The localization error is measured at every possible receiver position in the case of LoS link, noiseless overall link (including NLoS link and LoS link), and noisy overall link (including NLoS link, LoS link, and ambient noise), based

Table 3 Details for the distribution of SNR and Ricean K factor.

Parameters	SNR		Ricean K factor	
	Ratio/dB	Coordinate/m	Ratio/dB	Coordinate/m
Maximum	23.54	(1.6, 1.6)	20.54	(2.5, 2.5)
Minimum	18.94	(0.1, 0.1)	10.64	(0.1, 0.1)
Average	22.45		15.98	

on the least squares method using the parameters listed in Table 2. The simulation steps are as follows: (1) select a point as the location of receiver and calculate the Euclidean distance between the receiver and the transmitters; (2) apply distances and parameters in Table 1 to the mathematical model shown in Eq. (1) and add Gaussian noise and diffuse signal power, which has already been evaluated in Sec. 4.2, in order to simulate received signal power gained by the detector in a realistic situation; (3) use Eq. (2) to calculate the estimated distances between the receiver and the four transmitters; (4) calculate the estimated coordinates of receiver by calling the least squares method function; (5) calculate the derivation between the real position and the estimated position of the receiver; (6) repeat steps from (1) to (5) and calculate the values of localization error at every possible position for receiver.

As seen in Fig 5(a), the localization error is almost zero if there is no noise or NLoS component in the room. To investigate the relation between the localization error and the NLoS component, the distribution of Ricean K factor, shown in Fig. 4, needs to be considered together. For noiseless overall link, the main factor that controls the localization accuracy is the NLoS signal power absorbed by the detector. Figure 4(b) shows that the diffuse signal has a smallest fraction at the room's center. Thus, it results in a minimum localization error of 0 cm at (2.5, 2.5, 0.85), as shown in Fig. 5(b) and Table 4. As a user moves to the walls, the localization error gradually increases and reaches the maximum localization error of 1.33 m at (0.1, 1.0, 0.85). Considering that the FOV is assigned as 65 deg in this system, the detector placed in the nearby corners can only receive LoS signals from the three nearest transmitters and less NLoS signals, which causes a step-wise descent of the localization error. Otherwise, if the FOV is >70 deg in this system, the detector placed in the nearby corners can receive LoS signals from all the four transmitters and more NLoS signal power. Thus, the maximum value of localization error occurs at the corners in this circumstance, which agrees with the result in Fig. 4(b), and the Ricean K factor is the maximum at the same coordinate.

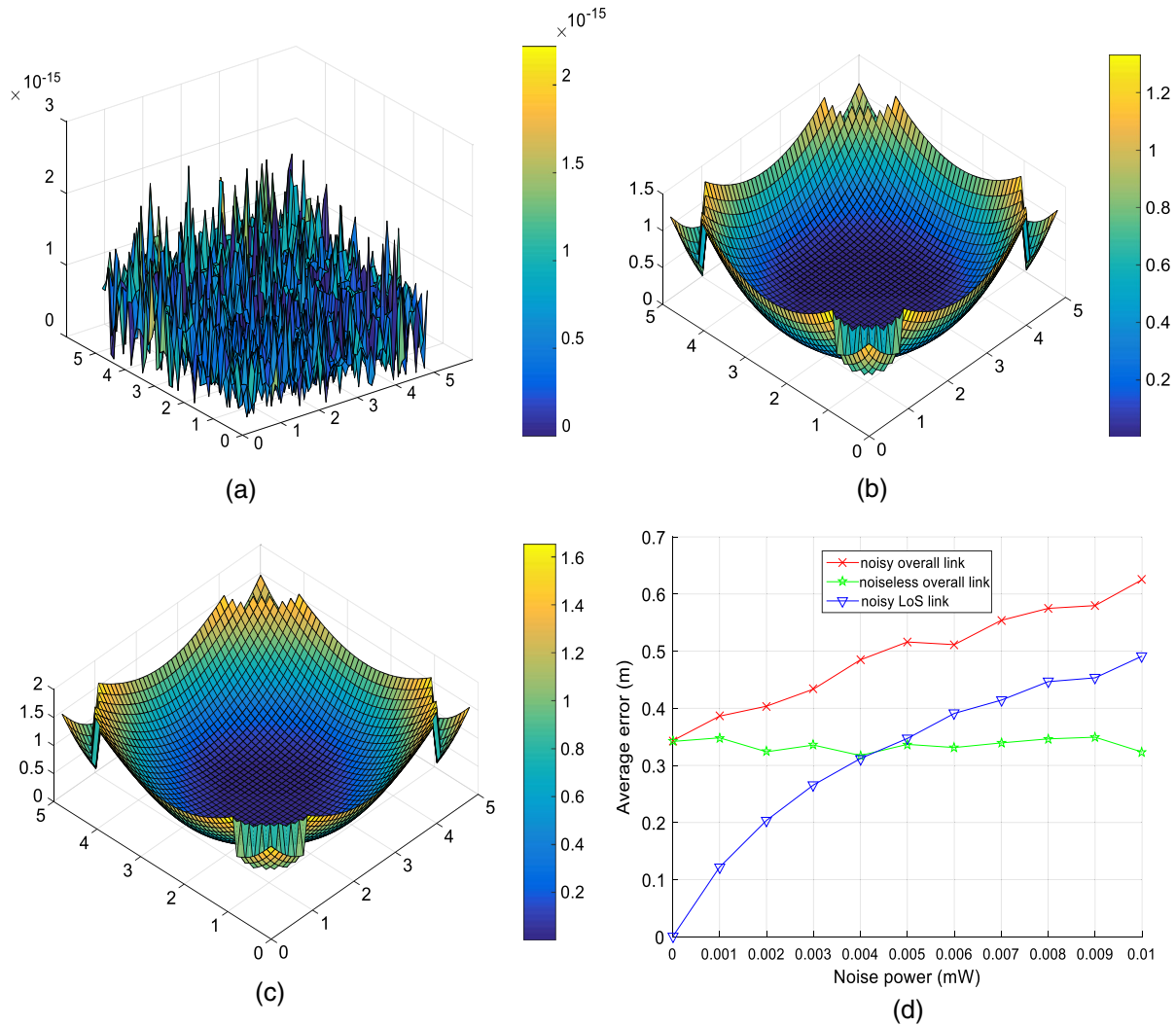


Fig. 5 Localization error distribution for (a) LoS link, (b) noiseless overall link, (c) noisy overall link, and (d) average localization error for different links.

Table 4 Details of the localization error from three different links.

Parameters	LoS link		Noiseless overall link		Overall link	
	MMSE/m	Coordinate/m	MMSE/m	Coordinate/m	MMSE/m	Coordinate/m
Maximum	2×10^{15}	(3.6, 3.6)	1.33	(0.1, 1.0)	1.65	(0.1, 1.0)
Minimum	0	(1.2, 1.2)	0	(2.5, 2.5)	0	(2.5, 2.5)
Average	0		0.32		0.61	

For the noisy overall link, the addition of noise causes the average error to rise up to 60 cm. Worst performance is obtained at places nearby the walls, and only 40% of the central areas maintain an error below 40 cm, as shown in Fig. 5(c). The minimum localization error is still situated at the center of the room (2.5, 2.5, 0.85), and the worst scenario is obtained at (0.1, 1.0, 0.85). Table 4 presents some details from Fig. 5. Furthermore, the average localization errors of the noisy overall link, noiseless overall link, and noisy LoS link for different noise levels are shown in Fig. 5(d). Both

NLoS signal power and noise received by the detector contribute to the average localization error in the noisy overall link. Since the noise power raise up to 0.004 mW, the average error in the noisy LoS link is large than that in the noiseless overall link, which indicates that the NLoS signal power is no longer the main error source in this scenario.

4.5 Effects of Environmental Parameters

In the overall link, the power of diffuse signals depends on the environmental parameters in the configuration, such as

the transmitter power, wall reflectivity, and receiver FOV. Thus, to diminish the localization error, some parameters can be adjusted according to the increase of Ricean K factor in the NLoS link.

First, we investigate the effect of the transmitter power on the localization error at different values of noise power in the overall link. As shown in Fig. 6(a), the localization error levels off to 6 cm as the transmitter power approaches 1 W, whereas it increases up to 0.4 m when the transmitter power is as low as 200 mW, at the noise power of 0.01 mw. Both LoS power and NLoS power enhance with the increase of transmitter power, which leads to the rise of SNR (and invariance of factor K). The localization error decreases because of the rising SNR.

Figure 6 demonstrates the average localization error for the overall link at different wall reflectivity at the noise power of 0.01 mw. According to Fig. 6(b), it shows that the lower wall reflectivity ($\rho = 1\%$) can yield a relatively smallest localization error (8 mm) when the transmitter power is 1 W per LED, whereas the error increases to ~ 0.16 m at a higher wall reflectivity ($\rho = 50\%$). More

optical signals are reflected by the walls and becomes the NLoS components. Thus, the performance of the localization system is degraded because of the increase of K factor (and invariance of SNR). However, in a room with smaller reflectivity, indoor temperature changes considerably during the day. Therefore, the balance between reducing localization accuracy and maintaining indoor temperature stability needs to be considered.

The FOV determines the vision of the optical instrument. If the visible light signal exceeds this angle, the optical sensor device at the access point cannot receive this signal, so the receiver FOV must satisfy the following criterion:

$$Fov \geq \arccos\left(\frac{h}{d_{\max}}\right), \tag{13}$$

where d_{\max} is the distance between a receiver and a LED. In an accurate localization process, the AP should be able to receive signals from at least three transmitters, and thus the FOV of the receiver needs to be >61 deg in this configuration, which guarantees that the least squares process can be

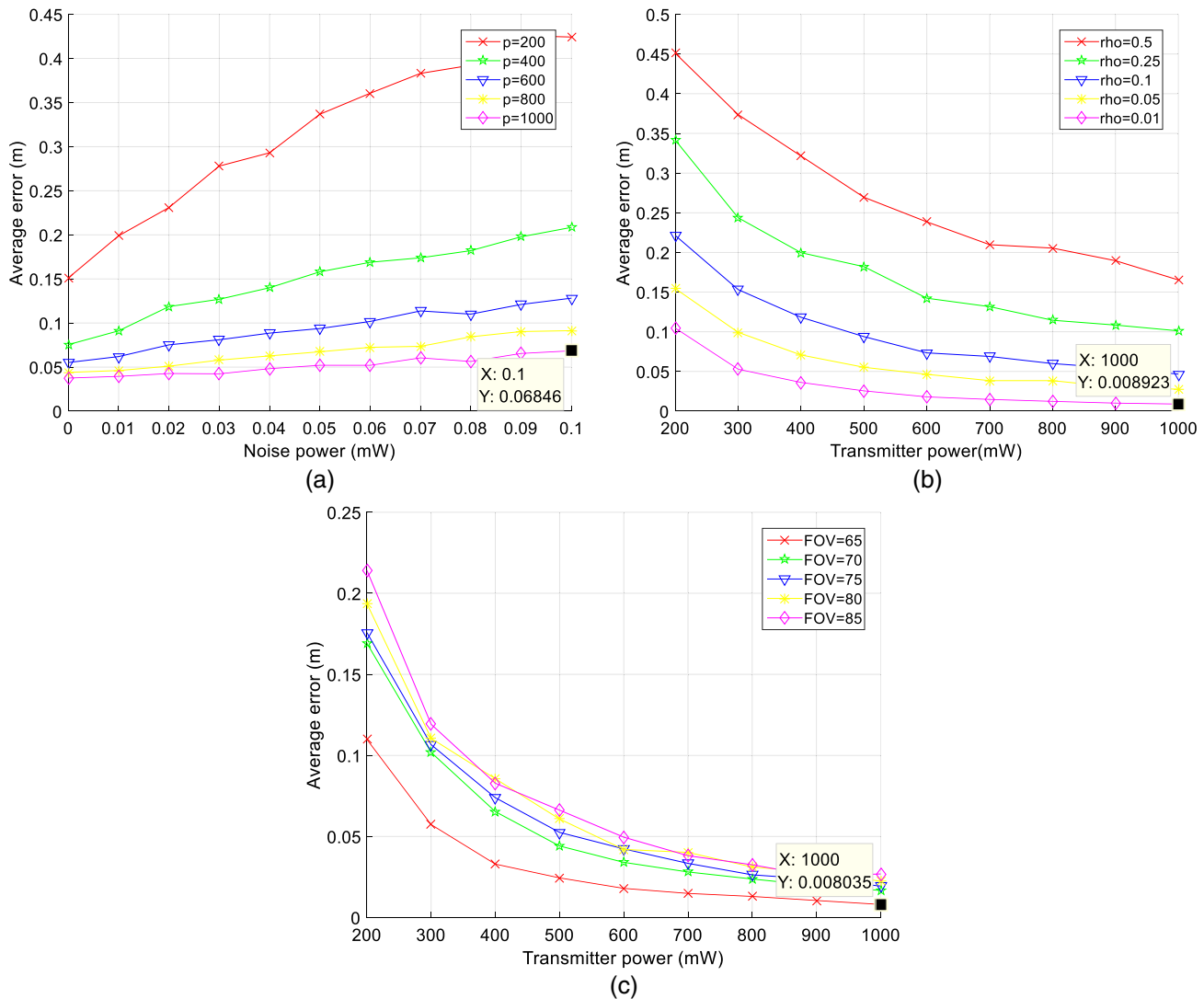


Fig. 6 Average localization error for different (a) wall reflectivity, (b) transmitter power, and (c) receiver FOV in the overall link.

Table 5 The comparison of the results in VLC localization systems.

Author	System model	Type of link	SNR (dB)	Ricean K factor (dB)	Localization error (cm)
The proposed work	$5 \times 5 \times 3 \text{ m}^3$	Noisy overall	35	25	0.8
Mohammed et al. ²⁴	$5 \times 5 \times 3 \text{ m}^3$	Noisy overall	40	4.3	68
Hosseiniyanfar et al. ²²	$5 \times 5 \times 3 \text{ m}^3$	Noisy overall	50	5.6	5
Elkarim et al. ²⁰	$5 \times 5 \times 4 \text{ m}^3$	Noisy overall	42	6.3	9.6
Mousa et al. ²⁵	$5 \times 5 \times 3 \text{ m}^3$	Noisy overall	25	13.5	4
The proposed work	$5 \times 5 \times 3 \text{ m}^3$	Noiseless overall	Noiseless	25	0.5
Gu et al. ²⁶	$6 \times 6 \times 3.5 \text{ m}^3$	Noiseless overall	Noiseless	6.3	8
Lim et al. ²⁷	$6 \times 6 \times 4 \text{ m}^3$	Noisy LoS	15	LoS link	10

employed at the worst scenario in the room. In addition, when the FOV of equipped PD is <67 deg, the localization system partially degrades to a three-transmitter system if the receiver is located at the corners. Figure 6(c) depicts the performance of average localization error with transmitted optical power per LED for the overall link at different FOV values at the noise power of 0.1 mW. The results show that larger FOV leads to the decrease of K factor (and invariance of SNR), which causes a larger localization error. When the FOV is assigned values from 61 deg to 67 deg, the localization accuracy of this system is 10 mm when the transmitter power reaches 1 W at the noise power of 0.1 mW. In conclusion, an optical sensor device with FOV = 65 deg is appropriate to be used in this configuration, which can provide an average error of <8 mm.

4.6 Comparison and Analysis

To evaluate the proposed localization system, in which the same RSS technique and least squares method are used, a comparison of the results with other localization systems is required. The configuration and accuracy for each previous work are listed in Table 5. The summary is divided into noisy scenarios or noiseless scenarios by the amplitude of the noise power, and the scenarios are further separated into LoS links and overall links by the amplitude of the Ricean K factor. Note that the configurations conducted in each work are different from each other. For a fair comparison, we introduce the Ricean K factor to indicate the relative value of the NLoS signal power in each system. Since none of the papers have investigated it before, we calculate the Ricean K factors by using the environmental parameters given in each work and present them in the table.

For the noiseless overall link, in Ref. 26, localization error was 8 cm at a Ricean K factor of 6.3 dB, whereas in the proposed system, the average localization error can be 0.5 cm at a Ricean factor of 25 dB. For the noisy overall link, the results in the previous work showed that the average localization error decreases as the Ricean K factor increases. For instance, in Ref. 24, the error was 68 cm at a Ricean K factor of 4.3 dB, whereas in Ref. 20, the error was 10 cm at a Ricean K factor of 6.3 dB. Note that the SNR were almost the same in these two systems. On the other hand, the results

of the previous works also showed that the average localization error decreases as the SNR increases. For instance, in Ref. 22, the average localization error was 5 cm at a SNR of 50 dB, whereas the error in Ref. 20 was 9.6 cm at a SNR of 42 dB. Note that the Ricean K factors in the two systems were almost the same. However, in our work, the error can be 8 mm, at a SNR of 35 dB and a Ricean K factor of 25 dB. At the end of this comparison, we can conclude that the localization error is inversely proportional to the amplitude of SNR and Ricean K factor. Owing to a higher SNR and Ricean K factor, the proposed system in the noisy overall link can provide a higher accuracy when compared to the reported works so far.

5 Conclusions

This work investigates the effect of NLoS signal on the accuracy of VLC indoor localization systems based on the RSS technique. In the system configurations, the diffuse signal power increases the total received power of VLC signals at the detector in the room from 1.8 to 1.85 mW. This derivation of received power results in a localization error of 0.5 m all around the room on average. To determine the relation between the localization error and the NLoS signal power, Ricean K factor has been introduced to evaluate the quality of localization. An upper bound is derived for the localization error that is inversely proportional to Ricean K factor at any receiver position. In addition, SNR is another parameter which impacts the localization accuracy. The worst localization performance (1.65 m) in the overall link is obtained at the walls with low values of K factor and SNR ($K = 12$ dB, SNR = 20 dB), whereas the best performance (0 m) is achieved at the center with the maximum K factor ($K = 20$ dB, SNR = 23 dB), which suggests that positions with better quality of communication (higher Ricean K factor and SNR) can improve the quality of localization. To increase the accuracy of localization systems, the final simulations are performed to investigate three environmental parameters which can reduce NLoS signal power, including wall reflectivity, transmitter power, and receiver FOV. This work provides references of parameters for building an experimental demonstration for the VLC indoor localization system. The results of final simulations show that a VLC system equipped with high power transmitters ($P_T = 1$ W) and

a large FOV receiver (FOV = 65 deg) in a low reflectivity ($\rho = 0.01$) room can achieve a high localization accuracy of 8 mm. Finally, a comparison of the localization accuracy is made with the previous works, and the proposed localization scheme provides the better performance, owing to the high value of SNR and Ricean K factor.

Acknowledgments

This work was sponsored by the National Natural Science Foundation of China (NSFC) (61401360) and Fundamental Research Funds for the Central Universities (3102017zy026). We thank Professor Cheng for his help in this work. We thank colleague Yu Shengdai for his advice for writing. We would like to thank Editage (www.editage.com) for English language editing. We have no conflicts of interest to disclose.

References

- P. B. Ahl and V. N. Padmanabhan, "RADAR: an in-building RF-based user location and tracking system," in *Proc. 19th Annu. IEEE INFOCOM*, pp. 775–785 (2000).
- A. F. Molisch, "Ultra-wide-band propagation channels," *Proc. IEEE*, **97**(2), 353–371 (2009).
- H. Kim and J. Choi, "Advanced indoor localization using ultrasonic sensor and digital compass," in *Proc. Int. Conf. Control, Autom. and Syst.*, pp. 223–226 (2008).
- J. Yang et al., "EKF-GPR-based fingerprint renovation for subset-based indoor localization with adjusted cosine similarity," *Sensors* **18**(1) 318 (2018).
- J. Yang, Y. Li, and W. Cheng, "An improved geometric algorithm for indoor localization," *Int. J. Distrib. Sensor Networks* **14**(3), 155014771876737 (2018).
- P. Müller, H. Wymeersch, and R. Piché, "UWB positioning with generalized Gaussian mixture filters," *IEEE Trans. Mob. Comput.* **13**(10), 2406–2414 (2014).
- P. Davidson and R. Piché, "A survey of selected indoor positioning methods for smart-phones," *IEEE Commun. Surv. Tutorials* **19**(2), 1347–1370 (2017).
- B. Zhu et al., "Three-dimensional VLC positioning based on angle difference of arrival with arbitrary tilting angle of receiver," *IEEE J. Sel. Areas Commun.* **36**(1), 8–22 (2018).
- B. Mungamuru and P. Aarabi, "Enhanced sound localization," *IEEE Trans. Syst. Man Cybern. Part B (Cybern.)* **34**(3), 1526–1540 (2004).
- M. F. Keskin, O. Erdem, and S. Gezici, "Cooperative localization in hybrid infrared/visible light networks: theoretical limits and distributed algorithms," *IEEE Trans. Signal Inf. Process. Networks* **5**(1), 181–197 (2019).
- Z. Xiao, H. Wen, and A. Markham, "Non-line-of sight identification and mitigation using received signal strength," *IEEE Trans. Wireless Commun.* **14**(3), 1689–1702 (2014).
- J. Wang et al., "Physical-layer security for indoor visible light communications: secrecy capacity analysis," *IEEE Trans. Commun.* **66**(12), 6423–6436 (2018).
- T. Q. Wang et al., "Position accuracy of time-of-arrival based ranging using visible light with application in indoor localization systems," *J. Lightwave Technol.* **31**(20), 3302–3308 (2013).
- M. S. Islam et al., "Indoor positioning through integration of optical angles of arrival with an inertial measurement unit," in *Position Location & Navig. Symp. (PLANS)*, pp. 802–807 (2012).
- J. Armstrong, Y. A. Sekercioglu, and A. Neild, "Visible light positioning: a roadmap for international standardization," *IEEE Commun. Mag.* **51**(12), 68–73 (2013).
- Q.-L. Li et al., "Three-dimensional indoor visible light positioning system with a single transmitter and a single tilted receiver," *Opt. Eng.* **55**(10) 106103 (2016).
- G. Shi et al., "A robust method for indoor localization based on visible light communication," in *IEEE Int. Conf. Comput. and Commun. (ICCC)*, pp. 2154–2158 (2017).
- H. S. Kim et al., "An indoor visible light communication positioning system using a RF carrier allocation technique," *J. Lightwave Technol.* **31**(1) 134–144 (2013).
- H. Huang et al., "Iterative positioning algorithm to reduce the impact of diffuse reflection on an indoor visible light positioning system," *Opt. Eng.* **55**(6), 066117 (2016).
- M. A. Elkarim et al., "Exploring the performance of indoor localization systems based on VLC-RSSI, including the effect of NLoS components using two light emitting diode lighting systems," *Opt. Eng.* **54**(10), 105110 (2015).
- T. Komine and M. Nakagawa, "Fundamental analysis for visible-light communication system using LED lights," *IEEE Trans. Consumer Electron.* **50**(1), 100–107 (2004).
- H. Hosseinianfar et al., "Positioning for visible light communication system exploiting multipath reflections," in *IEEE Int. Conf. Commun. (ICC)*, pp. 1938–1883 (2017).
- C. Tepedelenioglu et al., "The Ricean K factor: estimation and performance analysis," *IEEE Trans. Wireless Commun.* **4**(2), 799–810 (2014).
- N. A. Mohammed and M. A. Elkarim, "Exploring the effect of diffuse reflection on indoor localization systems based on RSSI-VLC," *Opt. Express* **23**(16) 20297–20313 (2015).
- F. I. K. Mousa et al., "Indoor visible light communication localization system utilizing received signal strength indication technique and trilateration method," *Opt. Eng.* **57**(1), 016107 (2018).
- W. Gu, M. Aminikashani, and M. Kavehrad, "Indoor visible light positioning system with multipath reflection analysis," in *IEEE Int. Conf. Consum. Electron. (ICCE)*, Las Vegas, Nevada, pp. 89–92 (2016).
- J. Lim, "Ubiquitous 3D positioning systems by LED-based visible light communications," *IEEE Wireless Commun.* **22**, 80–85 (2015).

Ge Shi is a PhD candidate at Northwestern Polytechnical University, Xi'an, China. She received her MS degree in information and communication engineering from Northwestern Polytechnical University in 2016. Her current interest includes visible light communication and physical layer security.

Yong Li is a professor at Northwestern Polytechnical University. His current interest includes digital signal processing and radar signal processing.

Wei Cheng is an associate professor at Northwestern Polytechnical University. His current interest includes internet of things and internet of vehicles.

Limeng Dong is a PhD candidate at Northwestern Polytechnical University. He received his MS degree in information and communication engineering from the Northwestern Polytechnical University, in 2014. His current interest includes physical layer security and cognitive radio network.

Junhua Yang is a PhD candidate at Northwestern Polytechnical University. His current interest includes indoor localization.

Wenjie Zhang is a PhD candidate at Northwestern Polytechnical University. His current interest includes massive MIMO and compressed sensing.